

FPGA-based Layered/Enhanced ACO-OFDM Transmitter

Qibing Wang¹, Binhuang Song¹, Bill Corcoran^{1,2}, David Boland¹, Leimeng Zhuang¹, Yiwei Xie¹, and Arthur J. Lowery^{1,2}

¹Electro-Photonics Lab., Dept. Elec. & Computer Sys. Eng., Monash University, Wellington Road, Clayton VIC3800, Australia

²Centre for Ultrahigh-bandwidth Devices for Optical Systems (CUDOS), Australia
arthur.lowery@monash.edu

Abstract: We present an FPGA-based QPSK-encoded 9.375 Gb/s layered/enhanced ACO-OFDM transmitter giving a high spectral efficiency. The measured Q-factor is greater than 13 dB after 20-km standard single-mode fiber transmission.

OCIS codes: (060.4510) Optical communications; (060.4080) Modulation.

1. Introduction

Optical orthogonal frequency division multiplexing (O-OFDM), also known as discrete multi-tone (DMT), is gaining more attention in short-haul optical communication systems due to increasing bandwidth requirements of data centers. In contrast to long-haul optical fiber links using external modulation and coherent detection, intensity modulation and direct detection (IMDD) using directly modulated lasers (DML) is preferred in short-haul optical systems due to its lower cost [1]. Several real-time DC-biased OFDM (DCO-OFDM) transmission experiments using field-programmable gate arrays (FPGA) have been demonstrated for short-haul optical fiber links [2-4]. However, DCO-OFDM is not power efficient, because the dominant unmodulated component of the light does not carry any information. Asymmetrically clipped optical OFDM (ACO-OFDM) [5] improves the energy efficiency of optical OFDM; however, because it sacrifices half of its spectral efficiency, it requires either the bandwidth of the electrical and optical devices to be doubled, or higher-order constellations requiring higher signal to noise ratios to be used. Recently, layered/enhanced asymmetrically clipped OFDM (L/E-ACO-OFDM) has been proposed, simulated [6-8] and experimentally demonstrated (using offline processing) [9] to improve the spectral efficiency of ACO-OFDM towards that of DCO-OFDM, while still maintaining a power advantage. As prior demonstrations used off-line digital signal processing (DSP), it remains to be seen how practical DSP hardware implementation issues may affect system performance.

In this paper, a 9.375 Gb/s FPGA-based QPSK-encoded L/E-ACO-OFDM transmitter is demonstrated. All the DSP functions are implemented in a FPGA chip and a MICRAM DAC is used to generate the laser drive signal. A Q-factor of 13.4 dB is measured after 20-km standard single-mode fiber (S-SMF) transmission.

2. L/E-ACO-OFDM Algorithm

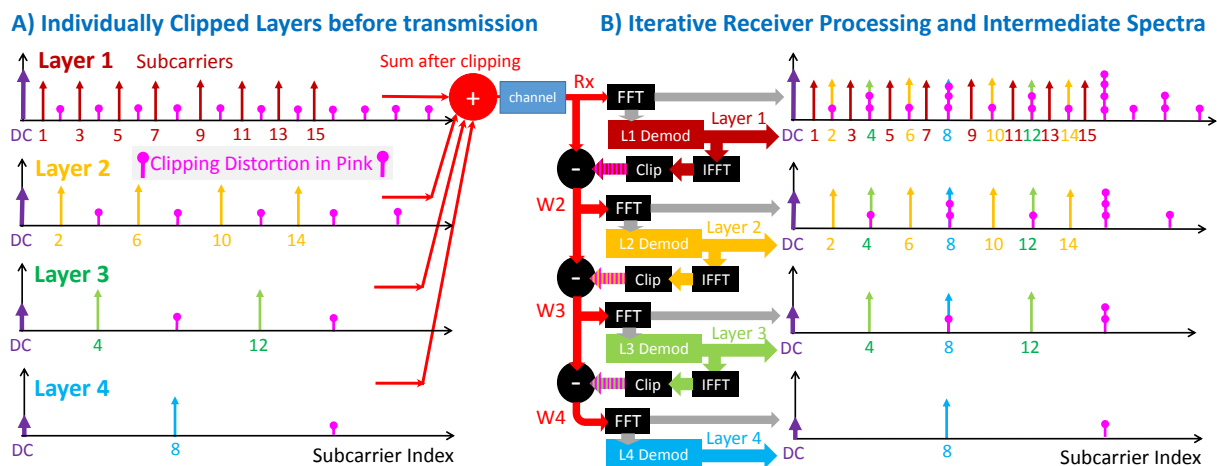


Fig. 1: Data-carrying subcarrier allocation in an L/E-ACO-OFDM transmitter (left) and iterative decoding (center) and spectra (right).

In an ACO-OFDM (ACO hereafter) transmitter, the distortion generated by clipping the signals below their mean level falls only on where even subcarriers should be; thus, only the odd subcarriers can be used to carry information, reducing its spectral efficiency by half. L/E-ACO-OFDM (EACO hereafter) allows the even-frequency subcarriers to be used, by adding a clipping distortion cancellation algorithm in the receiver. This removes the odd subcarriers of Layer 1 and their clipping distortion from the even frequencies. Thus the even subcarrier frequencies can be

allocated for data transmission. However, not all of the even frequencies are available in the Layer 2, only the $2 \times \text{odd}$ subcarriers, because their clipping distortion will fall on $2 \times \text{even}$ frequencies. Further layers are required to occupy some of the remaining even frequencies.

The procedure is illustrated in Fig. 1. Each layer, L (1, 2, 3, 4), uses a unique set of subcarriers which have frequency indices $2^{(L-1)}(2n+1)$, where $n = 0, 1, 2, 3, \dots$. Each layer generates a superposition of its subcarriers using an inverse fast Fourier transform (IFFT); then the negative values of this layer's waveform are clipped to become zero-valued. The spectra of each layer are shown on the left of Fig. 1. Finally, the already-clipped waveforms of all layers are combined to achieve a unipolar signal output (top right spectrum). Importantly, the clipping distortion from higher layers does not fall upon the data-carrying subcarriers in lower layers, thus Layer 1 can be decoded first, using a FFT and a slicer. As shown in the top-middle of Fig. 1, a facsimile of Layer 1's transmitted waveform can be regenerated with an IFFT and a clipper, and subtracted from the received waveform, to reveal the subcarriers (and clipping distortion) of the higher layers (called W2). Layer 2 is next decoded, and its distortion subtracted from W2, to reveal Layer 3 and 4. More details of the algorithm in the receiver can be found in [6-8].

3. Experimental Setup

Four layers were used with a 128-point IFFT in the first layer. As the time domain signals in high layers are periodic [7], the FFT size in high layers can be reduced by $2^{(L-1)}$, with $L = 1, 2, 3, 4$. Therefore, the FFT sizes in the four layers were 128, 64, 32, 16. The subcarriers in the four layers were 16, 8, 4, 2, so there were 30 subcarriers in total. Four layers gave 93.75% (30/32) of the spectral efficiency of DCO-OFDM.

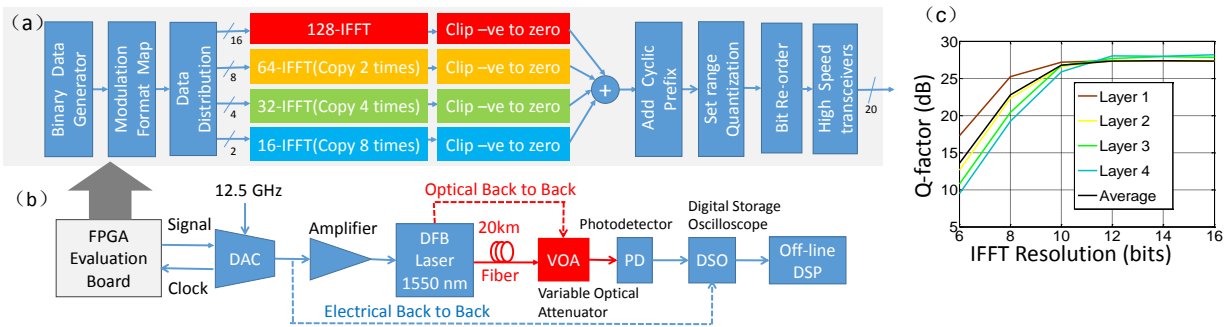


Fig. 2: (a) DSP functions in the FPGA; (b) EACO transmitter; (c) Simulated Q-factor versus IFFT resolution.

The EACO transmitter DSP functions performed in the FPGA are shown in Fig. 2(a). For this experiment, the test data and two training symbols were stored in the FPGA. Every clock cycle, 60 data bits were mapped to 30 QPSK symbols, each with N -bit resolution. Afterwards, these 30 complex numbers, combined with their Hermitian counterparts, were distributed to four layers through a data distribution module.

The IFFT resolution N was carefully examined to compromise between computational accuracy and hardware resource use. The signals after set-range and quantization module were then used to analyse the Q factor versus different IFFT resolutions, as shown in Fig. 2(c). This graph illustrates that a 12-bit IFFT resolution is sufficient to obtain the desired Q-factor. Furthermore, through reducing the resolution to $N=12$ -bits the entire design could fit onto the FPGA. Of the available resources on the Vertix-6 FPGA (XC6VLX240T), the design used 21% of the slice registers (64080), 44% of the slice LUTs (67317) and 83% of the DSP48E1s (640).

The 128 12-bit real outputs from each of the IFFT modules were then clipped to remove all negative values in each layer, before being added together. Finally, a 32-sample cyclic prefix (CP) was appended to the front of every OFDM symbol, producing 160 positive 12-bit words. The set-range and quantization module transformed this into 160 5-bit words which were distributed to 20 high-speed transmitters of the FPGA, representing four 5-bit parallel data streams to feed the MICRAM DAC.

The experiment setup of EACO transmitter is shown in Fig. 2(b). A 156.25-MHz clock generated by the DAC provided a clock to the FPGA, which was used to control all the DSP modules in the FPGA and synchronize the FPGA and DAC. The FPGA's high speed transmitters were programmed to have a data rate of 6.25 Gb/s; the four 5-bit parallel output streams from the FPGA were sampled by the 5-bit DAC at a sampling rate of 25 GS/s when clocked at 12.5 GHz. Since 30 subcarriers are used to carry QPSK mapped data, the overall net data rate is 9.375 Gb/s ($2 \times 25 \times 30 / 160$), neglecting an overhead of two training symbols.

4. Experimental Results

Firstly the electrical back to back performance of the EACO transmitter was evaluated by connecting the DAC output directly to a real-time Digital Storage Oscilloscope (DSO-X92804A) with an 80-GS/s sampling rate. The

captured samples were analyzed by off-line DSP in MATLAB. As shown in Fig. 3, the Q-factors for all the four layers are almost the same, which means that the clipping distortion is substantially cancelled in the receiver. The Q-factor is around 23 dB, a reduction of around 3.5 dB compared with Fig. 2(c), due to the DAC noise.

Then the Q-factor performance for a back-to-back optical link was measured by directly connecting the laser output to a variable optical attenuator (VOA) as shown in Fig. 2(b). The peak-to-peak voltage (V_{pp}) of DAC analog output signal is 500 mV. Then the signals were fed through 18-dB attenuators and a DC block, followed by a 24-dB gain 40-GHz linear electrical amplifier (SHF-807). The resulting 1-volt (p-p) output was connected to a distributed feedback laser, which was biased at 33 mA. A 16-GHz photodetector (DSC-40S) was used to convert optical signals to electrical signals, which were then sampled by DSO and processed off-line in MATLAB. No optical attenuation was added by VOA in this experiment. As shown in Fig. 4(a), the average Q factor of optical back-to-back is around 20 dB, a reduction of 3 dB compared with electrical back-to-back. There is a 5-dB penalty for the highest-frequency subcarriers. Finally, the Q factor was evaluated again after transmission over a 20-km span of S-SMF. Without using any optical amplifier, the Q-factor calculated from the average BER is still above 13 dB as shown in Fig. 4(b). Note, however, that the higher-index subcarriers suffer a larger penalty of 13 dB, compared with the low-frequency subcarriers, most probably because of the interaction of laser chirp and fiber dispersion.

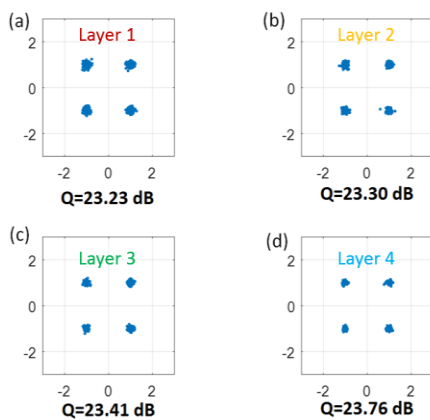


Fig. 3: Q-factor for electrical back to back.

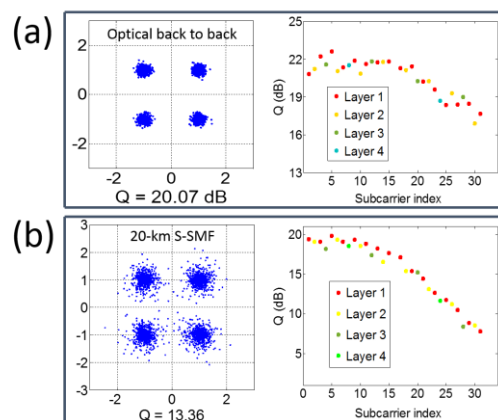


Fig. 4: Q factors: (a) Optical back to back. (b) 20-km transmission.

5. Conclusions

In this paper, the first FPGA-based QPSK-encoded EACO transmitter with a net data rate up to 9.375 Gb/s has been demonstrated using a DML. With off-line processing in the receiver using MATLAB, EACO signals are successfully transmitted over a 20-km span of S-SMF with a Q factor higher than 13 dB. In the future, bit and power loading could be used on the lower-frequency subcarriers to enhance the data rate.

Acknowledgements

This work is supported under the Australian Research Council's Laureate Fellowship scheme (FL130100041) and CUDOS – ARC Centre of Excellence for Ultrahigh bandwidth Devices for Optical Systems (CE110001018).

References

- [1] N. Cvijetic, "OFDM for next-generation optical access networks," *J. Lightw. Technol.*, vol. 30, no. 4, pp. 384-398, 2012.
- [2] Y. Benlachar *et al.*, "Generation of optical OFDM signals using 21.4 GS/s real time digital signal processing," *Opt. Exp.*, vol. 17, no. 20, pp. 17658-17668, 2009.
- [3] R. P. Giddings, *et al.*, "Experimental demonstration of a record high 11.25 Gb/s real-time optical OFDM transceiver supporting 25km SMF end-to-end transmission in simple IMDD systems," *Opt. Exp.*, vol. 18, no. 6, pp. 5541-5555, 2010.
- [4] M. Chen, J. He, and L. Chen, "Real-time demonstration of 1024-QAM OFDM transmitter in short-reach IMDD Systems," *IEEE Photon. Technol. Lett.*, vol. 27, no. 8, pp. 824-827, 2015.
- [5] J. Armstrong and A. J. Lowery, "Power efficient optical OFDM," *Electron. Lett.*, vol. 42, no. 6, pp. 370-372, 2006.
- [6] Q. Wang, C. Qian, X. Guo, Z. Wang, D. G. Cunningham, and I. H. White, "Layered ACO-OFDM for intensity-modulated direct-detection optical wireless transmission," *Opt. Exp.*, vol. 23, no. 9, pp. 12382-12393, 2015.
- [7] A. J. Lowery, "Comparisons of spectrally-enhanced asymmetrically-clipped optical OFDM systems," *Opt. Exp.*, vol. 24, no. 4, pp. 3950-3966, 2016.
- [8] M. S. Islam, D. Tsonev, and H. Haas, "On the superposition modulation for OFDM-based optical wireless communication," 2015 IEEE Global Conference on Signal and Information Processing (GlobalSIP), pp. 1022-1026, 2015.
- [9] B. Song, C. Zhu, B. Corcoran, Q. Wang, L. Zhuang, and A. J. Lowery, "Experimental Layered/Enhanced ACO-OFDM short haul optical fiber link," submitted to *Photonics Technology Letters*.